

Beyond the vision

Exploring the properties of the Atomic Force Microscope

Lab 2

**Department of Physics, University of Toronto Scarborough PHYC11:
Intermediate Physics Laboratory II**

Professor Dan Weaver

1. Mar. 2024

Table of content

<u>Table of content</u>	2
<u>Authors</u>	3
<u>Abstract</u>	4
<u>Introduction</u>	5
§ 1: The Limit of Light	5
§ 2: Atomic Force Microscopy	5
§ 3: Objectives	9
<u>Method</u>	10
§ 1: Apparatus	10
§ 2: Detecting unit	11
§ 3: Procedure	12
<u>Results</u>	14
<u>Discussion</u>	17
§ 1: Limitations of the constant force mode	17
§ 2: Limitations of the constant height mode	17
<u>Conclusion</u>	19
<u>References</u>	20

Authors

Ivan Pakhomov
Student number: 1008040013

Abstract

This paper discusses traditional microscopes' limitations due to light's diffraction limit and introduces Scanning Probe Microscopy (SPM) as a solution. Specifically, the paper focuses on Atomic Force Microscopy (AFM), which measures the force between the tip and the sample. The theoretical background of the forces involved in the tip-sample system, including the van der Waals force, is explored. The paper also explains the operation of an AFM and its various modes of operation. The focus of this experiment is on the contact operational modes of the microscope, which are constant force and constant height modes. The obtained results demonstrate the limitations of the two modes and show the capabilities of this field of microscopy. It was found that the biggest problem of scanning using the constant height mode is the vast amount of noise and sensitivity on the P, I and D controller values. The biggest limitation of the constant height mode was found to be the inability to scan the samples with the deep structures. Finally, the paper discusses the significance of AFM in various fields and its potential for future research.

Introduction

§ 1: The Limit of Light

Human beings experience physical phenomena through senses - sight, hearing, taste, touch, and smell. This enables the hearing of the frequency of oscillations of strings in musical instruments, tasting and smelling the combinations of various atoms into complex molecules, observing the emitted or reflected light, and sensing the texture through touch. These senses enable humans to understand the world and its physical properties. However, the senses have limitations like any detector. For instance, if one encounters an utterly black surface that perfectly absorbs any light that reaches it, how can he comprehend its properties? In such cases, when the material is non-hazardous, one uses the sense of touch to feel any bumps or valleys present, which helps them build their understanding of the material at hand.

When we want to explore things beyond our senses' range, we use technology to assist us. For example, we use microscopes when we want to look at tiny objects. These instruments have been around since the seventeenth century and are used to study objects that are millimetres or even micrometres in size. Microscopes use lenses to focus the light that reflects off the object onto the eyes or a light-detecting device. However, they have limitations since they rely on the properties of light.

The most significant limitation comes from the wave-like nature of light and is called the 'diffraction limit.' This limit occurs when light is reflected from two points a distance d apart, it interferes and combines into a single light wave, resulting in an inability to distinguish the points. For a light with wavelength λ , travelling in a medium with refractive index n and converging on a point with half-angle θ , Ernst Abbe found in 1873 that the minimum resolvable distance d is (Lipson et al., 1995, pp. 327-340):

$$d = \frac{\lambda}{2n \sin \theta} = \frac{\lambda}{2NA}, \quad (1.)$$

Where NA is the numerical aperture, which depends only on the properties of the microscope. The maximum numerical aperture for the visual microscopes is usually 1.40 (Abramovitz & Davidson). When the object is illuminated with blue light, it becomes impossible to see beyond 178 nanometres, which is equivalent to 0.17 micrometres. One way to reduce this distance is to use light with a shorter wavelength, but this can have an impact on the properties of the object of study since it results in the light wave having higher energy. In addition, detecting radiation with short wavelengths is much more complicated than that in the visible range.

The solution to this problem is to refer back to the example with the black surface and use the 'touch.' This method of studying objects beyond the diffraction limit is called Scanning Probe Microscopy (SPM). It relies on the interactions between the probe and the surface rather than on the reflected light.

§ 2: Atomic Force Microscopy

In 1981 and 1982, Binnig and Rohrer invented the Scanning Tunneling Microscope (STM), which earned them a Nobel Prize in 1986 (Voigtländer, 2019, p. 4). The STM works by applying a voltage between the probe and the conducting sample, causing a tunneling current to flow when the probe is moved closer to the sample. By measuring this current and changes in it as the distance between the tip and sample changes, the topographical map of the scanned surface can be created. The significant drawback of this instrument is that it can only scan conducting surfaces.

In 1985, Binnig invented the Atomic Force Microscope (AFM), which resolved this issue (Binnig et al., 1986). This type of microscope is the focus of this paper. It operates similarly to an STM, but instead of measuring the tunneling current, it measures the force between the tip and the sample. The subsequent sections focus on the theoretical explanation of these forces.

2.1 FORCES BETWEEN TIP AND SAMPLE

The force between the tip and the sample consists of long-range and short-range forces. One of the most vital forces in the tip-sample system is the van Der Waals force. This is the attractive force between neutral atoms and can be described as a spontaneous formation of fluctuating electric dipoles that attract each other (Voigtländer, 2019, pp. 161-176). This is a long-range force that has the interaction potential

$$U_{vdW}(r) = -\frac{C}{r^6} \quad (2.)$$

Where r is the distance between the tip and the sample, and C is the interaction constant. However, the fact that this is a long-range force and acts on all of the atoms in the volume of the tip and the sample needs to be accounted for. This can be achieved through integration and by approximating the tip as a sphere of radius R_{tip} , we get:

$$dU_{vdW} = -\frac{C\rho_{tip}\rho_{sample}}{|\mathbf{r}_{tip} - \mathbf{r}_{sample}|^6} dV_{tip} dV_{sample} \rightarrow U_{vdW} = -\frac{HR_{tip}}{6d}$$

Where ρ_{tip} and ρ_{sample} are the atom densities of the tip and the sample, $H = \pi^2 C \rho_{tip} \rho_{sample}$ is the Hamaker constant representing the strength of the van Der Waals interaction, and d is the tip-sample distance measured from the tip apex. Typical values of H are in the range of a few eV. Then, the force between the tip and the sample is

$$F_{vdW} = -\frac{\partial U_{vdW}}{\partial d} = -\frac{HR_{tip}}{6d^2} \quad (3.)$$

This is the largest force for distances larger than 1 nanometre.

In addition to the attractive van der Waals force, other forces need to be considered due to the quantum mechanical nature of atoms. Apart from attractive interactions such as chemical or metallic bonding, there is also a repulsive force that comes from the Pauli exclusion principle. This principle states that no two electrons can occupy the same state in an atom. As the tip approaches the sample, it initially experiences attractive forces. However, as it gets closer, the electrons in the inner closed-shell orbitals begin to interact, leading to a strong repulsive force. Both of these interactions can be modelled by the Lennard-Jones potential. This is the approximation model that serves to describe the interaction between two molecules, but it works equally well in the field of atomic force microscopy, as it is a commonly accepted interaction force in the AFM (Sarrid, 1994). This potential has the form:

$$U_{LJ} = 4\epsilon \left[\left(\frac{\sigma}{r} \right)^{12} - \left(\frac{\sigma}{r} \right)^6 \right] \quad (4.)$$

It models both the attractive van der Waals ($-1/r^6$ term) and the repulsive ($1/r^{12}$ term) potentials. Equation (4) ϵ represents the depth of the potential well and σ is the distance at which the potential is zero. Figure 1 shows the Leonard-Jones potential together with attractive and repulsive terms.

Figure 1 shows that the force (the negative gradient of the potential) is repulsive but turns attractive as soon as r becomes greater than σ .

There are certain forces that can cause errors while scanning that need to be taken into account. These factors are briefly mentioned here as they do not play a significant role in the experiment being discussed. When working in a medium like air, humidity is one of the factors that need to be considered. The varying humidity levels create a thin layer of water on the sample and tip, which can cause capillary forces

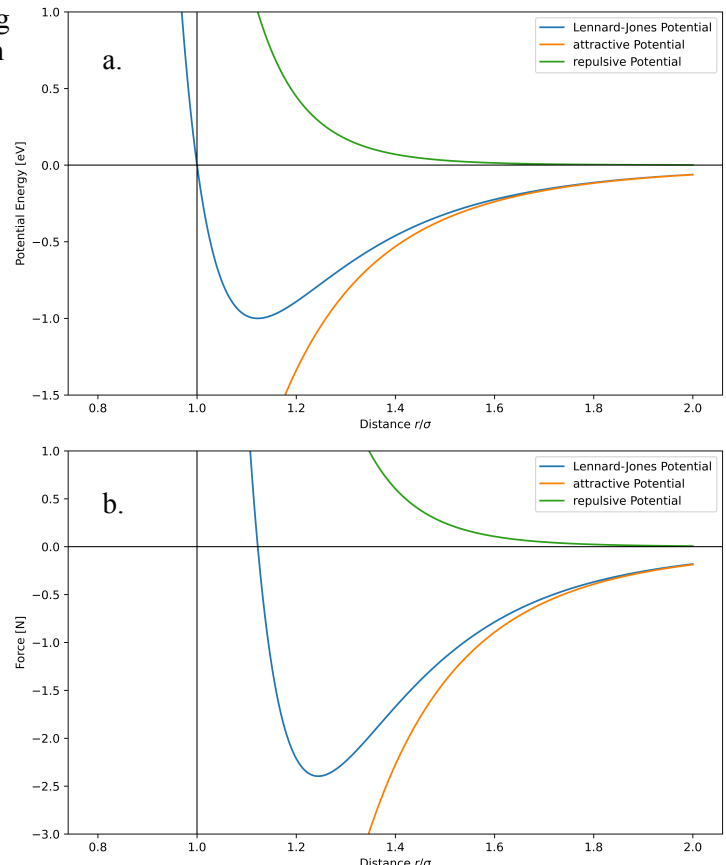


Figure 1. Lennard-Jones potential together with attractive and repulsive terms (a.) and the corresponding forces (b.) versus dimensionless distance r/σ

(forces that liquids exert on the substances during the contact) that might obstruct the readings. For further discussion, please refer to Zitzler et al. (2002). Another factor that could obstruct the work of the AFM is the snap-to-contact effect. This happens when the tip snaps onto the surface while approaching it. It can be compared to a magnet on a spring that is too close to a metal sheet, and the magnetic interaction between them becomes so large that the magnet snaps onto the sheet of metal and stays there. However, these effects are not discussed in our experiment as they are more relevant in a dynamic mode, as explained in section 2.2.2.

2.2 SCANNING MODES

There are two ways to scan a sample surface using the Atomic Force Microscope (AFM). However, before discussing these methods, the basic structure of the AFM must be reviewed. Figure 2 shows a schematic representation of the microscope's structure. The cantilever, which we have referred to as the tip, is shown, along with the sample that sits on top of the movable surface. The cantilever plays the role of an eye in the AFM in the sense that the scan of the surface is done by detecting the cantilever's bending. The piezo controls are used to move the scanning surface in the x, y, and z directions. The laser's reflection from the cantilever is detected by the position-sensitive detector, which processes the deflection of the tip in the z-direction. The detector then returns this information to the feedback electronics, creating a topology image and controlling the movement of the surface in the z-direction for the next step of scanning. Now, with a clear understanding of the structure of the AFM and its theoretical background, we are ready to turn our attention to the scanning regimes.

2.2.1 CONTACT MODE

The experiment discussed in this paper employed the first method of atomic force microscopy, which is the contact mode. In this mode, the tip maintains constant contact with the sample, and repulsive forces ($F > 0$ in Fig. 1 b) act on the tip as it moves along the sample surface using the x, y and z controls. By using the laser and a position-sensitive detector (as shown in Fig. 2), we can detect the deflection of the cantilever from its initial position according to Hooke's law (since the cantilever behaves like a spring). The contact mode is the simplest, in construction, mode since it does not require any additional mechanisms for balancing or adjustments, unlike the dynamic mode. Unfortunately, this simplicity has its drawbacks. Firstly, due to strong forces in this mode, the cantilever or the surface of the sample might be damaged since the atoms of both objects interact and their positions change due to the elasticity of the tip and the sample materials (for tip-sample contact mechanics, see Derjaguin et al. (1975)). Secondly, the resolving power is limited due to the tip-sample contact area, which does not allow atomic resolution. Taking both of these issues into account, this method satisfies the need to study the material when there is no interest in atomic structure.

Contact mode has two different operation modes, namely, constant force mode and constant height mode. In the contact height mode, the z-position of the tip is given by a balance of forces. When the cantilever comes close to a sample, the repulsive Lennard-Jones force starts acting on it, while the tip acts on the sample with the force given by Hooke's law. The measurement is taken by setting the initial deflection of the tip, which the feedback electronics maintain at the same level throughout the scanning, as shown in Figure 3. This operational mode allows for scanning the samples with deep surfaces while reducing the risk of damaging them. However, there are limitations to this mode of operation. To maintain a constant height, the feedback

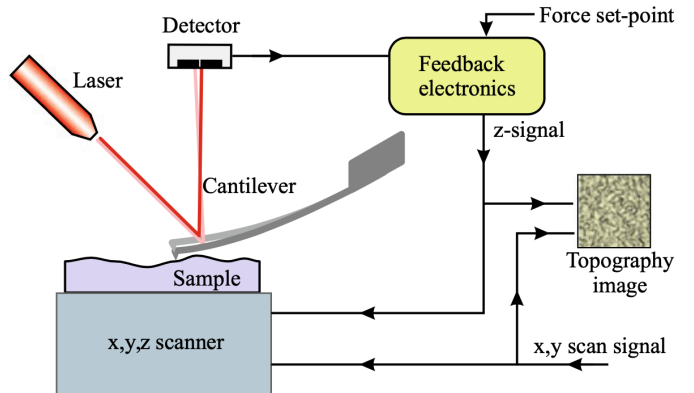


Figure 2. Schematics of the atomic force microscopy operation

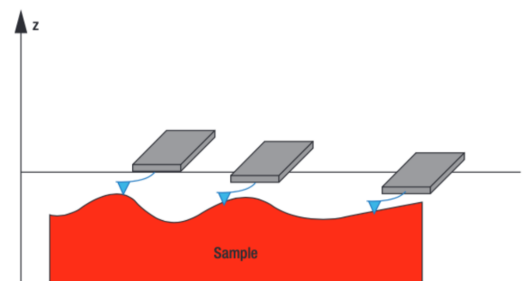


Figure 3. Functional principle of the constant force mode (taken from Feigl, 2012)

electronics continuously monitor the bending of the cantilever using three controllers: Proportional (P), Integral (I), and Derivative (D). The complete explanation of these controllers requires an understanding of the AFM electronic circuits, which unfortunately falls outside the scope of this paper. However, basic principles will be discussed, as they are important for understanding the operation of the constant height mode. These controllers are related to the error signals that arise due to the impedance of the numerous capacitors, inductors and resistors integrated into the circuits. This error signal is expressed as:

$$e = \omega - x(t)$$

Where ω is the set force, and $x(t)$ is the force exerted on the cantilever at time t. The feedback electronics calculate e and vary the height of the sample for the force to return to the set-point value. The controller P is proportional to this error by a factor K_P and allows the computer to do quick calculations of the height at which the sample needs to be raised or lowered to. However, it constantly overshoots the set value. The I and D controllers are related to e by an integral ($K_I \int_0^t e(\tau) d\tau$) and a derivative ($K_D \frac{de(t)}{dt}$), respectively, as their names suggest. They are used to correct the overshoot of the P controller as they are more precise. The major drawback of I and D is that they take a long time to process, and if the proportionality constants (K_P, K_I, K_D) are chosen incorrectly, the scanning might yield unusable results (Voigtländer 2019 pp. 99 – 105). Overall, the constant height mode yields accurate measurements and allows the scanning of the samples with large height differences unless the proportionality factors are chosen incorrectly, which results in a noisy image due to overshooting.

In contrast, in constant height mode, the initial height of the tip is maintained throughout the scanning, while the position-sensitive detector detects any deformations of the cantilever, i.e., bending or torsion. The significant drawback of this method is that it has certain height limitations. For instance, if the surface of the sample has deep valleys and the measurement starts off at a peak, it is impossible to detect anything at the bottom of the valley since the height will always remain the same. Fortunately, the constant force mode resolves this issue. On the other hand, the significant benefit of this mode is the lateral force scan, or the friction force microscopy (FFM). In the constant height mode, the measure of torsion of the cantilever can be obtained, which allows for a measurement of the material contrast by the difference in the friction coefficients. Figure 5 shows this process.

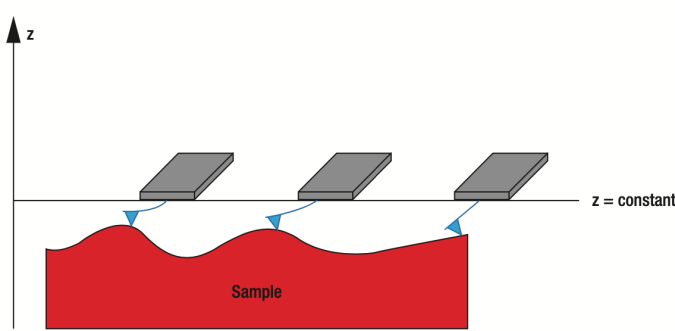


Figure 4. Functional principle of the constant height mode (Feigl, 2012)

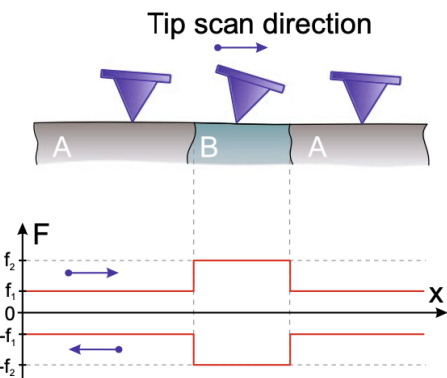


Figure 5. Difference in the friction signals on the materials with different friction coefficients, that is obtained by the FFM (Voigtländer, 2019. p. 204)

2.2.2 DYNAMIC MODE

The second technique that will be discussed briefly is dynamic atomic force microscopy. Unlike the contact mode, this technique works in the $F < 0$ regime in Fig. 1b. This method creates a topology map by oscillating the tip closely to its resonance frequency, so when the attractive forces start acting between the tip and the sample, the frequency and the amplitude change. By detecting these changes, we are able to build a topology map. This method allows for higher-resolution images up to the atomic scale. However, this measurement is much more sensitive compared to the contact mode. As

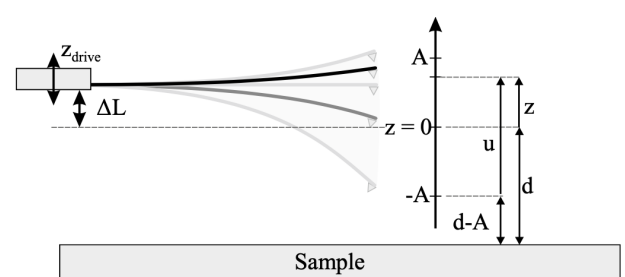


Figure 6. Schematic representation of the dynamic mode (Voigtländer, 2019. p. 262)

discussed in 2.1, the humidity of the air plays a significant role in this mode, as the capillary effect can cause significant errors in creating the topology map.

§ 3: Objectives

In the experiment, Thorlabs' EDU-AFM1(/M) Educational Atomic Force Microscope was used. It operated in contact mode to study different surfaces, such as a piece of vinyl record, a metal with nano-coating, and a microstructure sample. By taking the topographical maps of these surfaces, the microscope's abilities and limitations were explored. The primary goal of the experiment was to set the microscope up in operation mode and get a topological image of the sample surfaces at constant height and constant force.

Method

§ 1: Apparatus

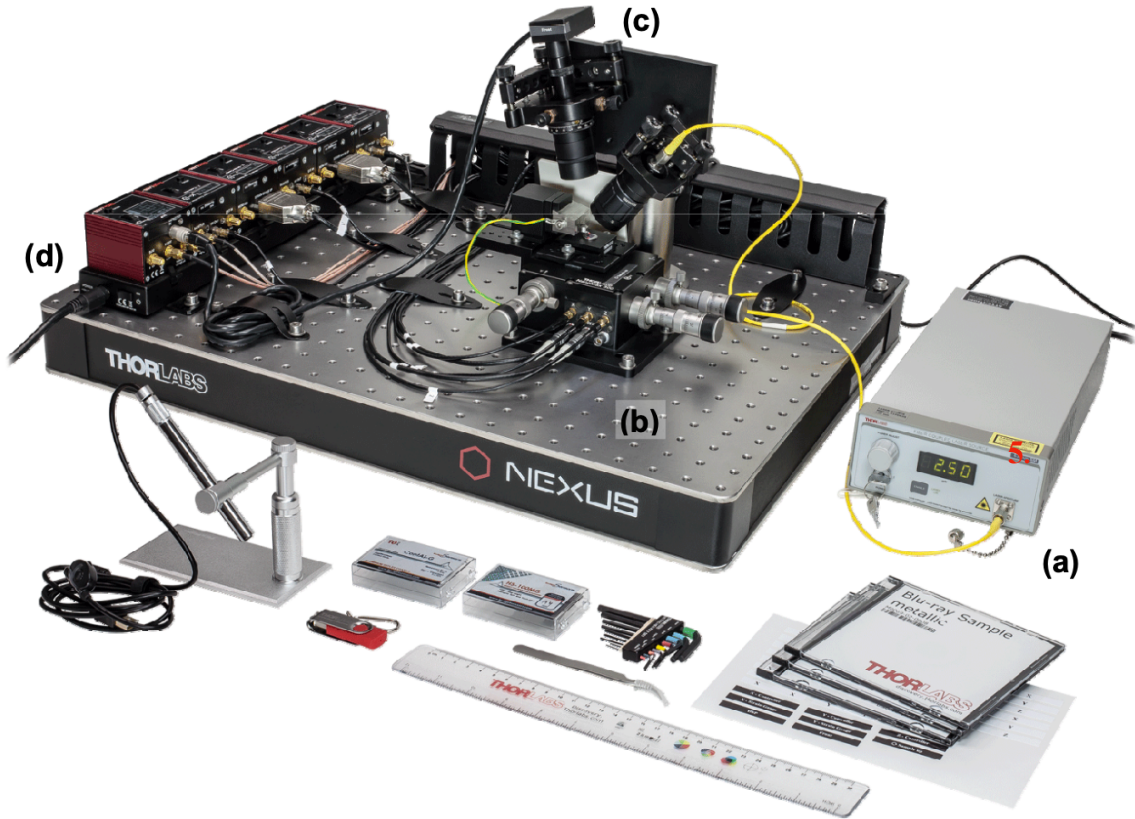


Figure 7. Thorlabs' EDU-AFM1(M) Educational Atomic Force Microscope Kit. (a) – Laser source; (b.) – positioning unit; (c.) – signal processor; (d.) – piezo controller with feedback controller.

In the experiment, the Thorlabs' EDU-AFM1(M) Educational Atomic Force Microscope was used. Figure 7 shows a picture of the AFM and the additional tools provided with it. Part (a.) shows the 635 nm laser source. The single-mode fibre (yellow wire) is used to transmit the laser from the source to the laser mount. Part (b.) is the positioning unit that helps to secure all the parts of the microscope in place. Part (c.) is a signal processor that is connected to the detector mount (the whole detecting unit, including the laser, the detector, the probe holder and the positioning unit, are described in the following section). Lastly, element (d.) consists of 3 piezo controllers (one per axis), two strain gauge controllers (for the x and y axes), and one photodiode controller and auto aligner. The piezo controllers control the position of the positioning unit while scanning. They measure the position in Volts. The limitations of the x and y piezo controllers are not of significant importance, as they just control the motion of the sample in the horizontal plane, and the scanning is primarily height, not position-dependent. However, the maximum and minimum outputs of the z-piezo controller are important for the measurement, as it is responsible for the distance between the tip and the sample. The z-piezo controller output varies from 0 V to 50 V, where 50 V represents the maximum height and 0 V represents the minimum height. The strain gauge controllers control the x and y piezo controllers during the measurements and dictate the step. The strain gauge controllers can be regarded as the brain that dictates x and y piezo controllers how to move. Lastly, the photodiode controller provides the readings from the position-sensitive signal processor (c.) in Figure 7 (detector in Figure 1). In addition to giving the readings, this element controls the z-piezo controller during the constant-force mode scanning.

§ 2: Detecting unit

Figure 8 shows the two views of the detecting unit: a profile picture (a.) and a top view (b.). This is the heart of the atomic force microscope, as the sample is placed at sample stage 2.) and scanned by the probe that has a cantilever. After the probe is placed in the probe holder, the laser from 3.) is adjusted so that it is reflected from the tip of the probe right into the detector on top of the detector mount 4.).

Figure 8b shows the coarse adjusters A, B, C, and D used to adjust the sample stage under the probe's tip before scanning begins. It is very important that these adjusters are centred to allow travel in all directions while scanning. Otherwise, this might cause significant problems while taking the measurements (see Results section).

The probe is the most important component of the AFM, as it interacts with the sample during the measurement process (as explained in §2 of the Introduction). The role of the probe is similar to that of the lenses in traditional microscopes. Therefore, it is crucial to have a clear understanding of its properties to comprehend the workings of the AFM. The following subsection focuses on the properties and characteristics of the cantilever.

2.1 CANTILEVER

Figure 9 shows the probe placed in the probe holder as seen under the microscope. Figure 10 shows the electric microscope images of the cantilever used in the experiment.

The specifications can be found in the datasheet provided by the manufacturer (<https://www.budgetsensors.com/contact-mode-afm-probe-contact>). The tip is made of silicon; its force constant is 0.2 N/m, so, according to Hook's law, the forces acting on the cantilever are

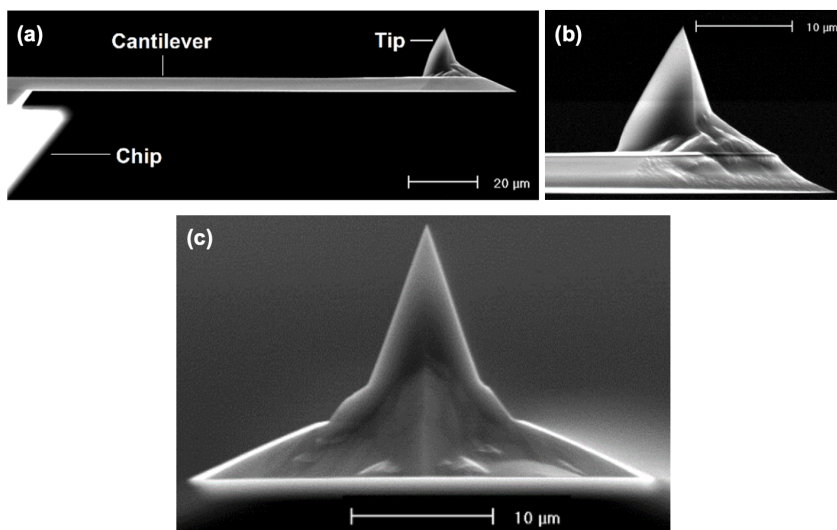


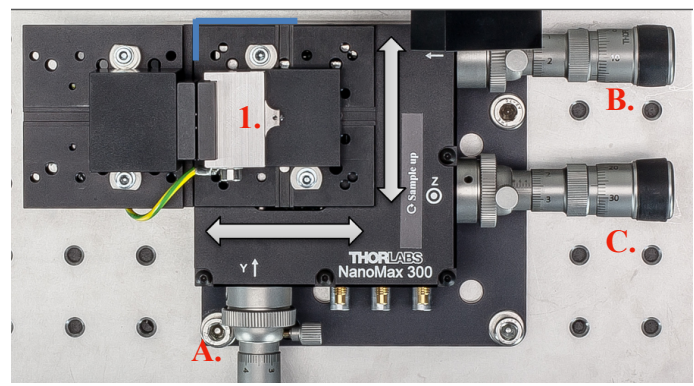
Figure 10. Electron microscope images of the cantilever used in a tip.

(a.) – overview; (b.) – side view of the tip; (c.) front view.

Taken from (<https://www.budgetsensors.com/contact-mode-afm-probe-contact>)



a.)



b.)

Figure 8. Detecting unit
a.) – Profile picture: 1.) – probe holder; 2.) – the sample stage; 3.) – laser mount; 4.) – detector mount; 5.) – the positioning unit.
b.) – View from above: A.) – y-axis coarse adjuster; B.) – x-axis coarse adjuster; C.) – z-axis coarse adjuster; 1.) – probe holder



Figure 9. The probe in the probe holder under the microscope

extremely small. In addition, the radius of the tip is only 10 nm, which allows for precise measurements. Besides the probe, it is equally important to discuss the work of the detector as it is the ‘eyes’ in this experiment.

2.2 DETECTING THE DEFLECTION

The deflection of the cantilever is measured by measuring the position of the reflected laser onto the detector Figure 7c. This detector is a four-segment photodiode that consists of silicon, and it can detect

wavelengths of 400 – 1050 nm. The spot size of the reflected beam plays a crucial role in measurements. It should not exceed the diameter of the photodiode (7.8 mm). Otherwise, it would preclude the measurement. Simultaneously, the spot size should be bigger than the spacing between the segments (0.2 mm). The datasheets (https://www.thorlabs.com/_sd.cfm?fileName=ETN033528-D03.pdf&partNumber=KPA101) recommend the laser spot size to be 1.0 – 3.9 mm in diameter.

To measure the tip's deflection, the laser spot has to extend across the quadrant limits. For instance, for XDIFF, it needs to be in the quadrant limits of Q1/Q2 to Q2/Q4. Figure 11 shows the calculations of the voltages proportional to deflection. Figure 12 shows the detector's readings, as seen in the software.

Now, we want to turn our attention to the experiment procedure.

$$\begin{aligned} \text{X-axis sensor: } & (Q_2 + Q_3) - (Q_1 + Q_4) \\ \text{Y-axis sensor: } & (Q_1 + Q_2) - (Q_3 + Q_4) \\ \text{SUM: } & (Q_1 + Q_2 + Q_3 + Q_4) \end{aligned}$$



Figure 11. Calculating the voltages on the photodiode

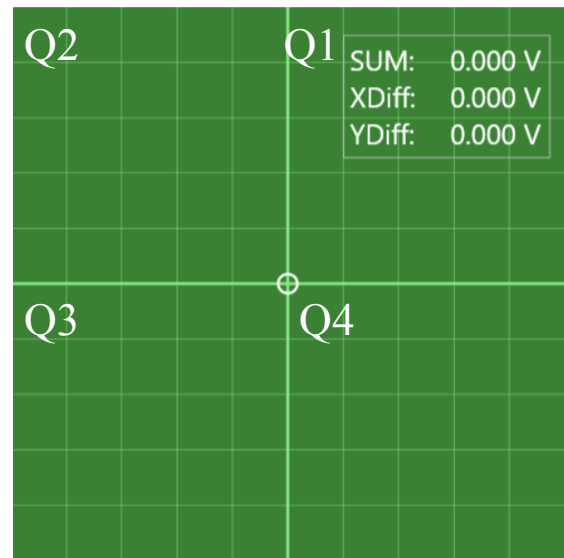


Figure 12. The readings off the detector by the software

§ 3: Procedure

In the experiment, the constant force and constant height modes were used to analyze the samples (as described in 2.2.1 of the introduction).

Before starting the measurements, the probe was installed in a probe holder. This was done manually and extremely carefully in order not to break a cantilever or a tip. After the probe was installed and secured, the laser needed to be adjusted to point directly at the cantilever (the red dot at the tip of the cantilever in Figure 9). This procedure was also manual and was done by first replacing the detector with the diffuser plate for direct observation of the reflected beam and then adjusting the positioners shown in Figure 13 until the reflection dot is centred, as in Figure 14. Then, the detector was reinstalled.

After all that initial preparation was finished, the detector mount was readjusted again so that the reflected dot was at $x = y = 0$, as shown in



Figure 14. The Reflection dot, adjusted on the center of the diffuser plate

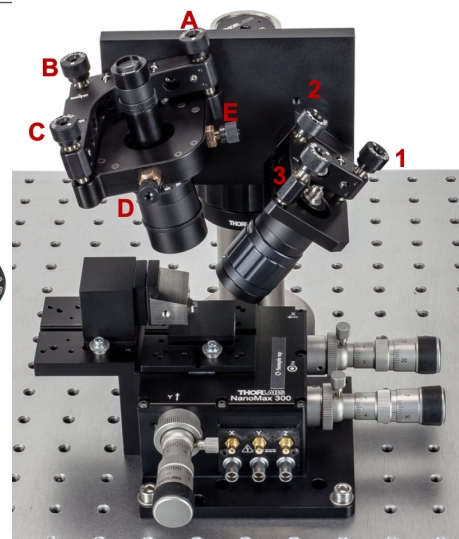


Figure 13. Adjustment of the beam path by means of the diffuser plate and kinematic holder. A to C are the angular positioners and D to E are the lateral positioners for the detector mount. 1 to 3 are the angular positioners for the laser mount.

Figure 12. Since we wished to work in the constant force and constant height modes, we needed to prepare the microscope for scanning.

For working in the constant force mode, the detector mount was readjusted so that the dot in the software appeared to be at XDIFF = -0.1 V. Then, the sample was placed under the probe, after which the probe holder was lowered using the z-axis coarse adjuster until the reading of the z-position showed 25 V. This corresponded to around $6.6 \mu m$ range in the z-axis. After all this was done, the scanning was started.

For working in the constant height mode, the procedure similar to the one described in the constant force mode was repeated so that the cantilever was in touch with the surface and the z-position showed 25 V. After that was done, the Z feedback had to be disabled (as shown in Figure 15) which retracted the tip from the surface. After that, using the z-axis coarse adjuster, we needed to put the tip onto the surface until we saw that the reflected dot had the x-position of 0.5 V. After all this was done, the scanning started.

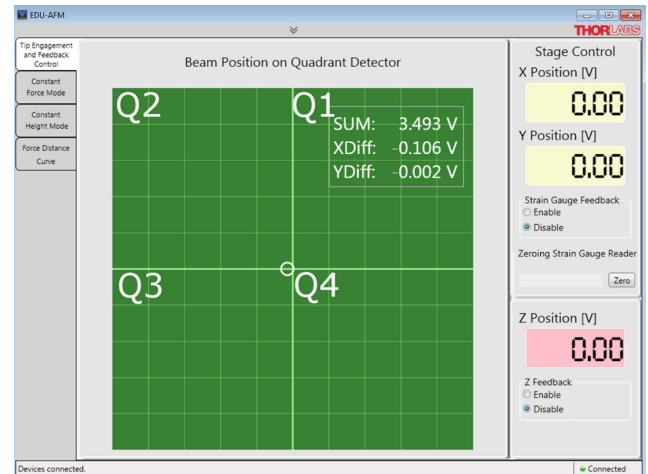


Figure 15. The software for scanning using the AFM

Results

The experiment was conducted in a room with 34% humidity and 22°C. The first step was to set the microscope in the operation mode (as described in §3 of the Method) and take the measurements of a piece of a vinyl record, a metal with the nano-coating and a microstructure sample. Figure 16 shows the surface of the sample with the nano-coating. This is the failed result that was not scanned along the y-axis (as seen by straight vertical lines). This figure shows the importance of correct adjustment of the coarse adjusters (as was mentioned in § 2 of the Method). When this issue was corrected, the measurements were taken using the constant force mode.

Figure 17 demonstrates one of the results obtained during the scanning. This particular image was chosen because it explicitly shows the noise caused by the incorrect choice of the P I and D values (2.2.1 of the Introduction). The scan was obtained by setting the resolution to 250×250 pixels and the scanning speed to 100 pixels per second. The scale of the x and y axes is 20 μm , and the scale of the z-axis is shown by the grayscale. The initial values of P, I, and D were set to 0.9, 1 and 0.7, respectively. After half of the scan was obtained, the P, I and D values were changed to 0.4, 0.599 and 0.2, and the scanning proceeded as before. The result is seen in Figure 17, and the change in the amount of noise on the image is apparent. Figure 19 represents the same data as in Figure 17 but in 3 dimensions (a.) and a slice of the data (1-pixel width) as seen from the x-axis (b.). These plots are discussed in detail in the Discussion.

Figure 18 was obtained in the constant height mode by scanning the sample with the microstructure. The resolution was set to 100×100 pixels, and the scanning speed was 60 pixels per second. Just as before, the scale of the x and y axes is 20 μm , and the z-axis scale is shown by the grayscale. Figure 19 (a.) presents the 3D plot of Figure 18; Figure 19 (b.) shows a one-pixel thin slice of the microstructure sample as viewed from the x-axis.

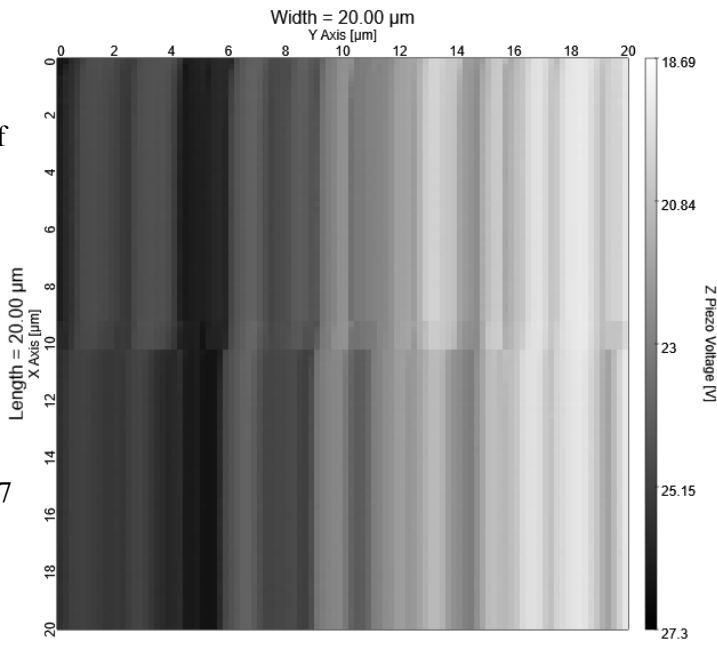


Figure 16. Failed scan of the sample with the nano coating, got in constant force mode

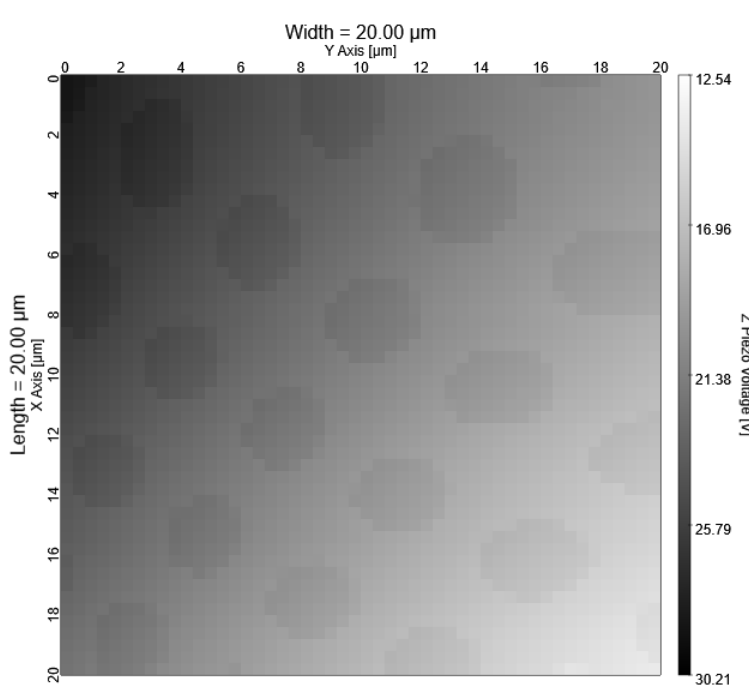


Figure 18. The microstructure sample. Result obtained in the constant height mode

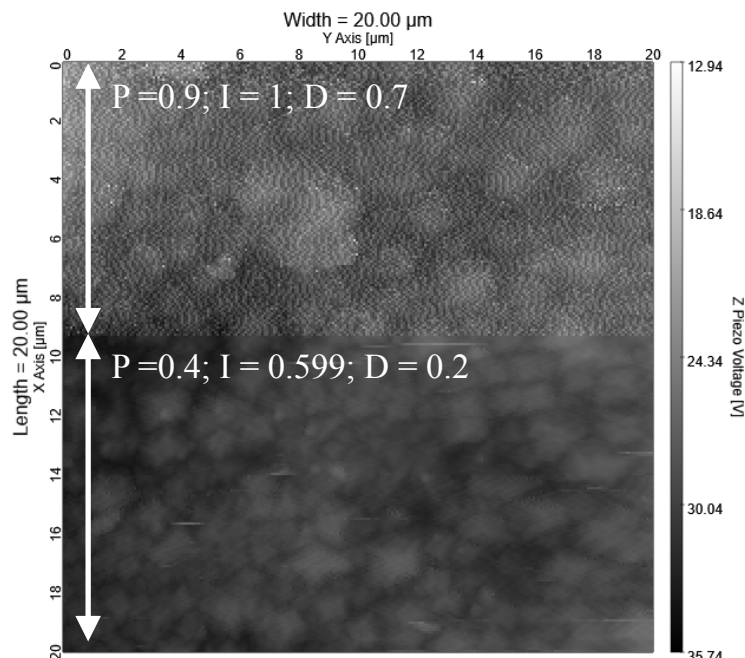


Figure 17. The scan of the sample with the nano coating. Obtained in the constant force mode. Demonstrated the influence of the P, I, D values on the obtained image

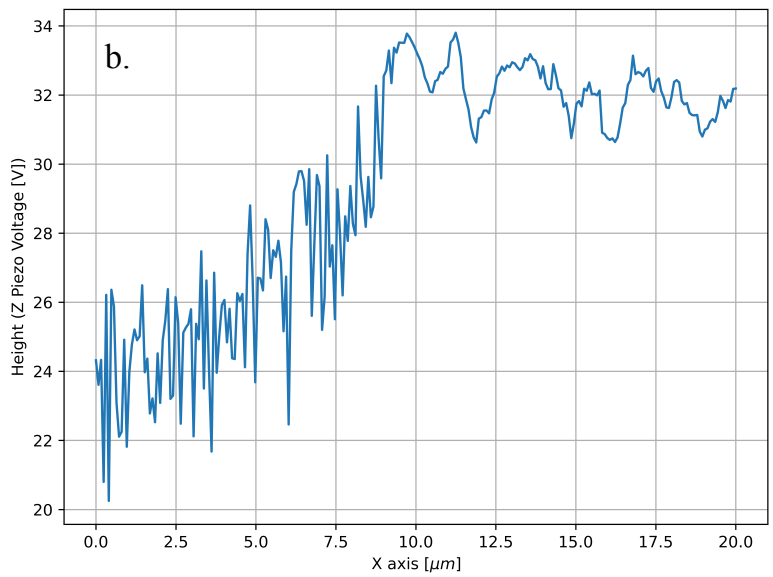
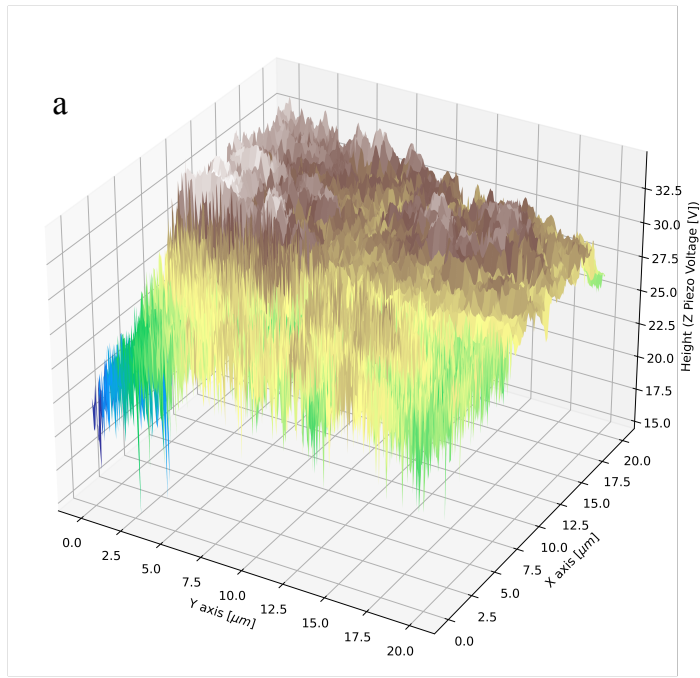


Figure 19. Plots of the data obtained by scanning the metal with the nano coating.
a.– 3D plot; b.– single-pixel width plot (view from the x-axis).

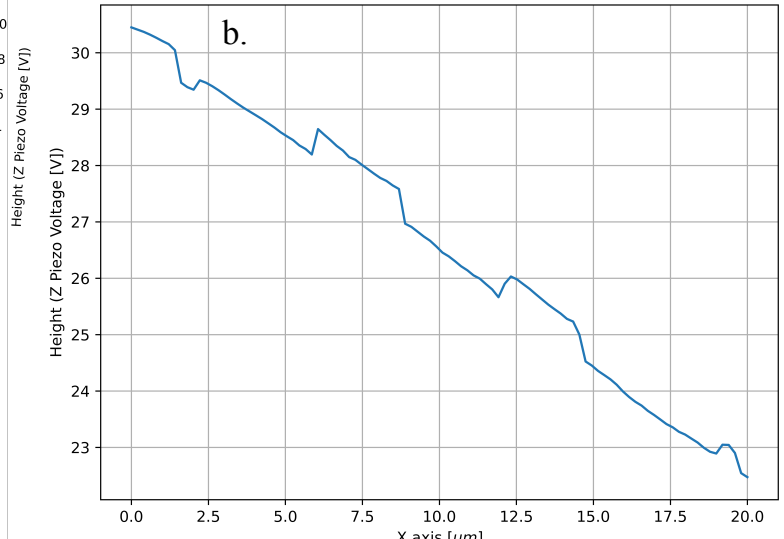
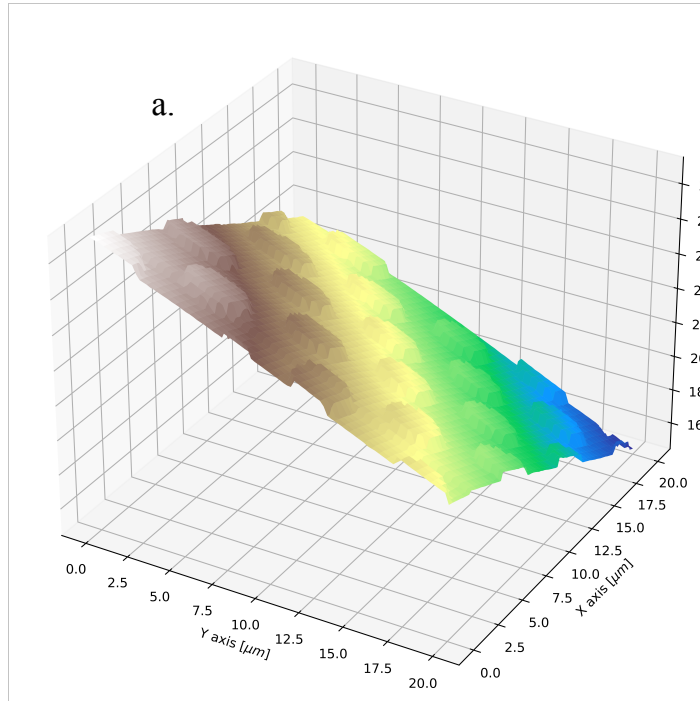


Figure 20. Plots of the data obtained by scanning the metal sample with the microstructure.
a.– 3D plot; c.– single-pixel width plot (view from the x-axis)

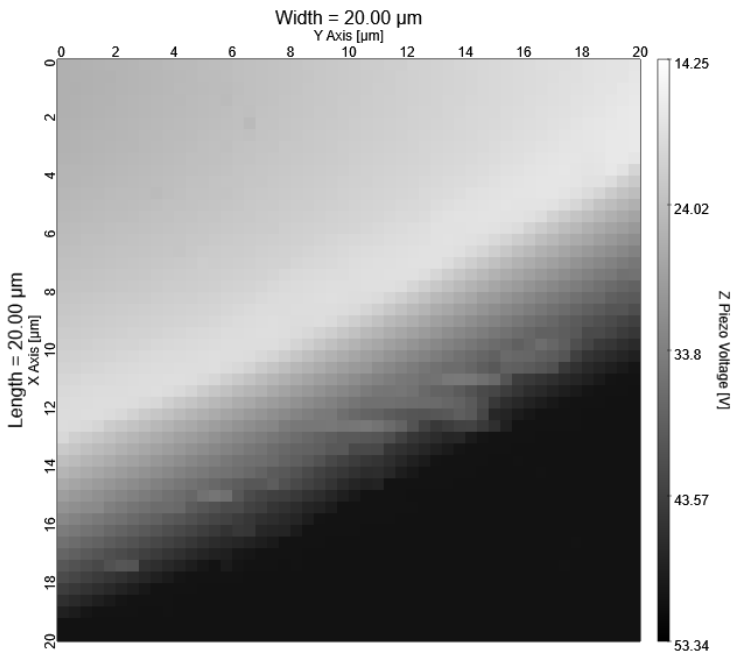


Figure 21. Piece of the vinyl record. Result obtained using the constant height mode

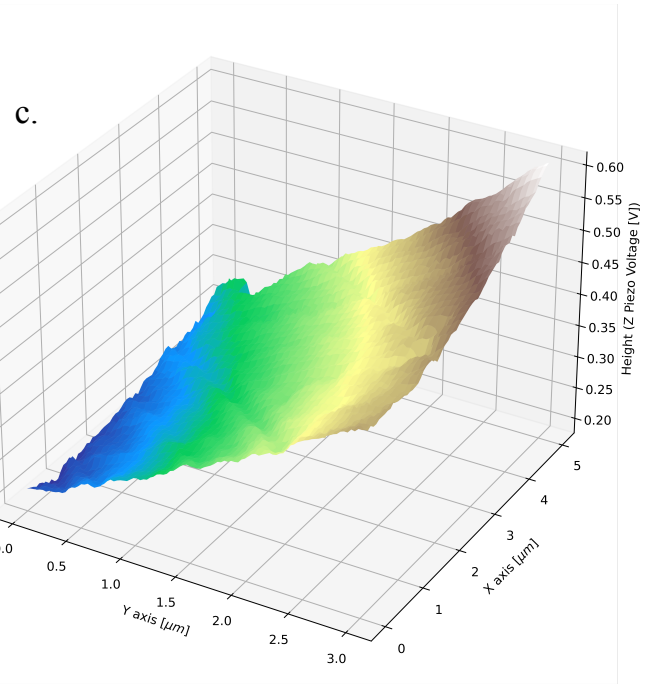
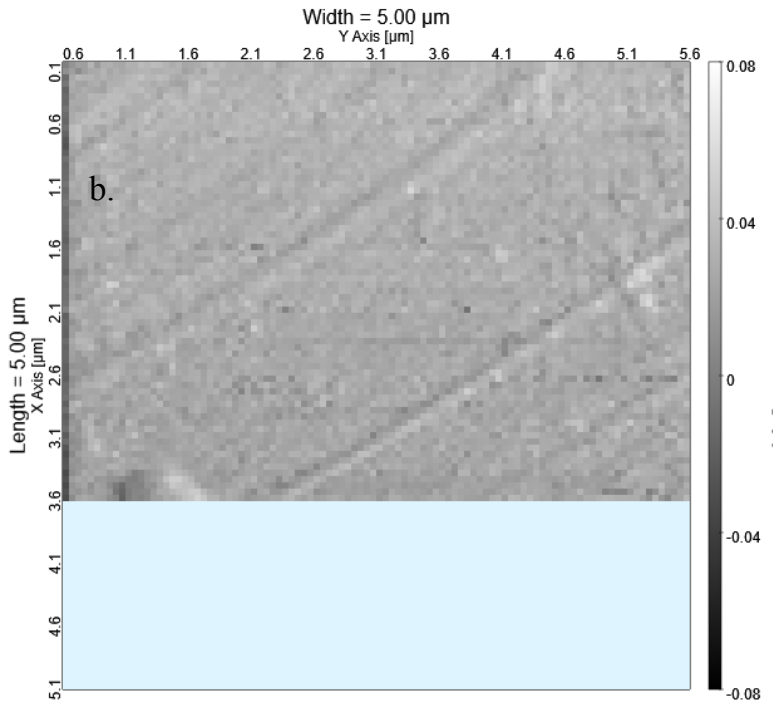
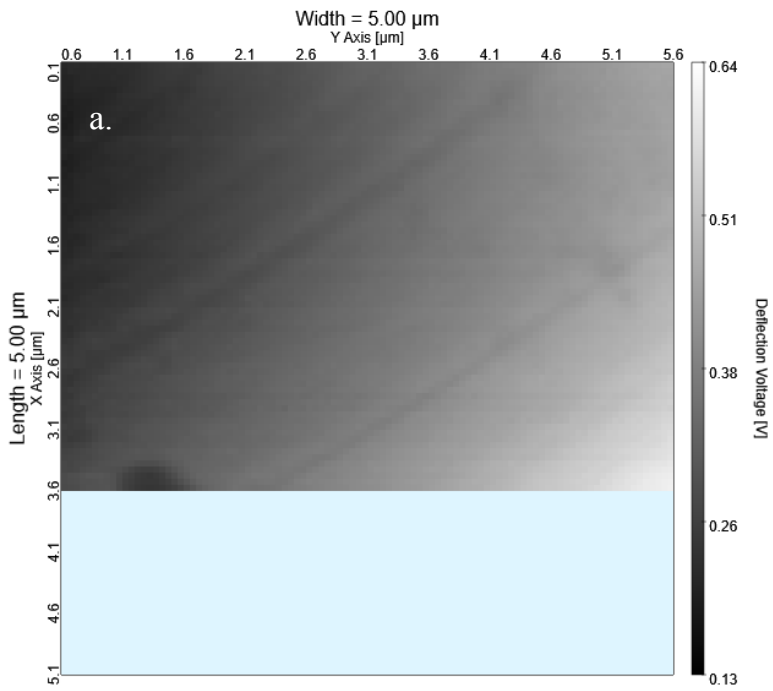


Figure 22. Piece of the vinyl record zoomed in down to a scale of $5 \mu\text{m}$, which shows the valley where the bumps create a sound.
a.– Obtained by a constant height mode; b.– Obtained by lateral force mode; c.– a 3D plot of a.

Figure 21 shows the scan of the piece of a vinyl

record. The image was obtained using the constant height mode. The resolution was set to 50×50 pixels, and the scanning speed was 50 pixels per second. The figure shows the ‘hill’ in between the tracks of the vinyl record. Later, the scan of the zoomed-in section of this piece of vinyl was taken, but in the region between the ‘hills’ (0 to $5 \mu\text{m}$ in Figure 20). This is the region where the tip of the vinyl player encounters ‘bumps’ and plays music. The topography map of this area is shown in Figure 22. Figure 22 (a) shows an image obtained in the constant height mode, with a resolution of 100×100 pixels and a scanning speed of 60 pixels per second. Figure 22 (b) shows the same region but scanned using the lateral force mode (and the same scanning parameters as (b)). The scales of the x and y axes are $5 \mu\text{m}$, and the scale of the z-axes is shown by the grayscale. Figure 22 (c) shows a 3D map constructed from the same data as Figure 22 (a). One thing worth noting is that Figures 22 (a) and (b) are not complete, and the scanning process stopped after $3.6 \mu\text{m}$. The possible reasons are discussed in the Discussion section.

Discussion

§ 1: Limitations of the constant force mode

Figures 17 and 19 present different plots of data obtained in a constant force mode of a piece of metal with the nano-coating. This nano-coating on the material creates the nano ‘bumps’ on the surface that are clearly visible in the lower part of Figure 17. The expected result of the scan was a monotone structure (such as in the lower part of Figure 17). However, as discussed in the Results section, the P, I and D values were changed in the middle of the scanning process (the initial and the final values of P, I and D were chosen arbitrarily), which resulted in a change in the amount of noise from the top to the bottom part. This drastic change is clearly visible in Figures 19 (a.) and (b.). The 3D plot (Figure 19 (a.)) shows the vast amount of noise appearing on the x-axis from 0 to around 9 μm . This noise prevents the nanostructure from being identified and might result in the incorrect interpretation of the obtained data. The reason for such drastic changes in the figure lies in the nature of the P I and D values.

As was discussed in section 2.2.1 of the Introduction, these values are responsible for identifying the height to which the tip should be raised or lowered, depending on the structure of the scanned sample. However, the incorrect choice of the speed of scanning and P, I and D values result in the appearance of unnecessary noises. To better understand this concept, one can take the example of a non-uniform black surface with a ‘step’ in the middle. In this case, constant force mode implies moving the entire hand instead of an individual finger when encountering an obstacle on the surface. When scanning the surface with one’s finger, one would start to raise their hand when they reach the step. However, they would only stop raising their hand once they have successfully moved past the step, but the brain takes time to stop the hand. As a result, a slight overshoot is happening (as shown in Figure 23), and the hand needs to be lowered to reach the top of the step. The process of the brain understanding that the finger is no longer touching the surface is similar to what is happening inside a computer when P, I and D values are calculated. The incorrect choice of these values results in a larger overshoot. These overshoots are clearly shown in Figure 19 (b.). Overall, the constant force mode is great for scanning surfaces with a deep structure. However, the sensitivity of the microscope to the choice of the P, I and D controllers makes this scanning mode vulnerable to the appearance of unnecessary and unphysical noises that might be corrected by repeating the scanning process with changed values.

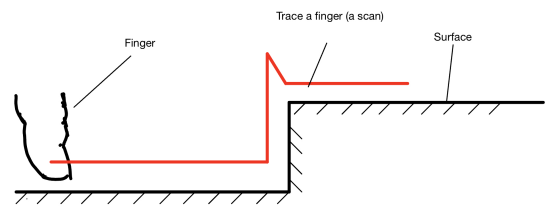


Figure 23 .Representation of the example of a scan of black surface using a finger.

§ 2: Limitations of the constant height mode

Figures 18, 20, 21, and 22 were obtained from the data received by scanning in the constant height mode. Figures 18 and 20 show the sample with the microstructure. This microstructure represents the circular ‘bumps’ around 2 μm in diameter (as seen in Figure 18). Figure 20 (a.) shows the 3D plot of the same data, and Figure 20 (b.) shows the one-pixel width cut as seen from the x-axis. There is no apparent noise present in these figures compared to the figures discussed in the previous subsection.

This is another demonstration that constant force mode is sensitive to the choice of the P, I and D values. However, there is another thing to notice about Figure 18. The ‘bumps’ should be perfectly circular and not be shaped like an oval, which we see in this figure. This phenomenon is explained by the incorrect choice of the scanning speed and the improper calibration of the microscope. The speed of the scanning plays an important role since the tip might ‘jump’ over some structures and show an unreal representation. In the case of this particular sample, Figure 20 (b.) shows that the edges of the ‘bumps’ are not the same in both directions (the scan was taken starting at $x = 20 \mu\text{m}$ and moving towards $x = 0 \mu\text{m}$). In this case, the tip ‘jumped’ over the left edges of the bumps. Another thing to notice about Figure 20 (b.) is that the edges are not vertical but tilted under the angle to the surface. The

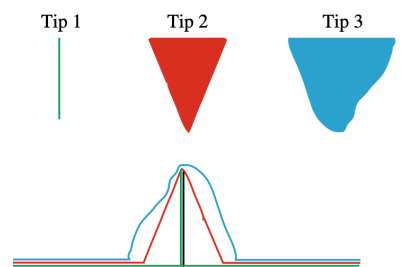


Figure 24. Representation of the dependance of the scan on the shape of the tip

explanation for this phenomenon lies in the form of the tip (Figure 24). As was discussed in section 2.1 of the Method, the tip has a pyramidal shape (Figure 10), which, in 2D, corresponds to Tip 2 in Figure 24. Thus, the slight tilt of the scan in Figure 20 (b.) is a tip-related artifact that can be removed only by changing the form of the tip.

Figures 21 and 22 show the plots of the vinyl record, the data for which was obtained in the constant height mode. All the limitations discussed in Figures 18 and 20 can also be related to the scan of the piece of vinyl. However, Figures 21 and 22 clearly show the main problem of the constant height mode—the inability to take precise scans of samples with deep structures. Figure 25 shows the structure of the vinyl record that was taken using the scanning electron microscope. The valleys where the audio information is contained are called the grooves (1. In Figure 25), and the hills that are used to lead the tip of the vinyl player are commonly referred to as the ‘dead wax’ or the ‘run-out grooves’ (2. In Figure 25). What is seen in Figure 21 is the edge of the dead wax (bottom right part). The top left part is empty because the scanning started from the hill, and the tip could not reach the bottom of the groove and take a scan. Figure 22 (a.) is a zoomed-in scan of the empty region in Figure 21. Figure 22 (b.) is the same region as 21 (a.) but obtained using a lateral force scan, and Figure 22 (c.) is a 3D plot of the data obtained from scan (a.). These three plots show the vinyl record's groove (1. in Figure 25). The tiny lines that are only $0.1 \mu\text{m}$ wide, which is beyond the diffraction limit of the visual microscopes, are clearly seen in each of the plots in Figure 22. These cuts are a result of the needle of a vinyl player cutting through the soft material. These lines can also be seen in Figure 25.

As was discussed in the Results section, these figures are not complete. The possible explanation for this defect lies in the limitations of the constant height mode. Recall from the Method section that the data is gathered by a light-sensitive detector that detects the reflection of the laser beam off from the cantilever. This means that if the laser does not point directly at the detector, the data is not gathered, and the scanning process cannot be complete. During the constant height mode, the data is produced by scanning the deflection of the cantilever from its initial position. This implies that if the cantilever is bent to the extent that the reflected laser beam stops pointing directly at the detector, the scanning process stops. This is exactly what happened while gathering the data for Figure 22. The cantilever reached the dead wax and was bent so that the reflected laser missed the detector, and the scanning was interrupted.

Lastly, both plots in Figures 20 (a.) and 22 (c.) are tilted with respect to the horizontal plane. In Figures 18 and 22 (a.), this is seen as a gradient from the top left part of the figures down to the bottom right part of the figures. This effect occurs from the surface of a sample being slightly tilted, which, in constant height mode, shows up as a gradient. Note that this effect is not observed in Figures 17 and 19, which were obtained using the constant force mode. This is because the force needed to be constant during the scanning process, so the tilt is accounted for.

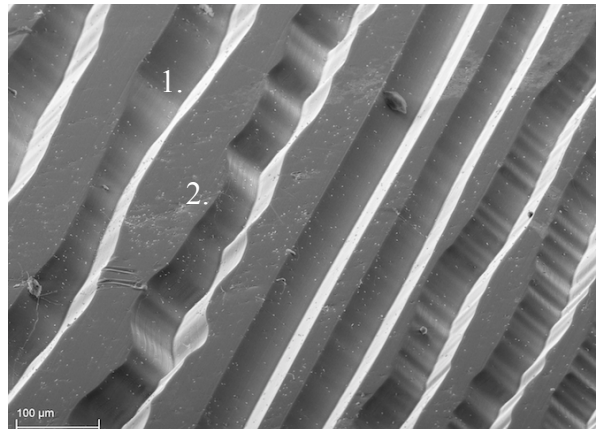


Figure 25. Image of the vinyl record under the microscope
1.—grooves; 2.—dead wax
(taken from <https://thevinylfactory.com/news/incredible-photos-of-record-grooves-under-an-electron-microscope/>)

Conclusion

This paper explores the working principles, abilities and limitations of the Atomic Force Microscope (AFM). It was created due to the inability of the visual microscopes to perform observation of samples smaller than 0.17 micrometres. As discussed, this is caused by the wave nature of the light and the diffraction that is attributed to all waves.

A clear parallel between the human touch and the working principles of the Atomic Force Microscopes was established. The AFM scans the samples to detect inconsistencies in their structure. The cantilever, which is used in the scanning process, can be compared to a human's finger in the sense that by touching a surface with a texture, one can identify and imagine what that surface looks like. This is the exact same process that the Atomic Force Microscope uses but on a drastically smaller scale. When one uses the word 'touch,' one implies direct contact with the surface. In reality, on the atomic scale, direct contact is impossible due to the strong repulsive forces that exist between atoms. This force is found from the Lennard-Jones potential (4.) and is used as a basis of Atomic Force Microscopy.

This paper focused on the AFM's contact modes, which were described as scanning modes. In these modes, the cantilever either maintained a constant height from the surface (constant height mode) or a constant force with the surface (constant force mode). In the constant height mode, the scans of the piece of vinyl record and of the sample with microstructure were obtained (Figures 18, 20, 21 and 22). In the constant force mode, the scan of the material with the nano-coating was obtained (Figures 16, 17 and 19).

The scan results showed that both constant force and constant height modes have limitations. The constant force mode is highly sensitive to the choice of the P, I, and D controllers, which results in the appearance of a vast amount of noise. This noise can only be reduced by repeating the scanning procedure with changed values of P, I, and D. However, it was discussed that the constant force mode allows the scanning of surfaces with deep structures, unlike the constant height mode.

The results of the scans using the constant height mode revealed four major limitations. First, this method cannot be used to scan surfaces with deep structures since the cantilever stays on the same height and might either brake if the force becomes too large or not finish the scan (as in Figure 22). Second, to obtain a good scan, the sample's surface should be completely horizontal. Otherwise, the scan will have a gradient or, in the worst-case scenario, the tip might break. Third, the shape of the tip and the scanning speed plays a significant role in the quality of the scan since tip artifacts create an altered scan that is not physical (Figure 25). Lastly, scanning in this mode might damage the surface of a sample that is softer than the tip material. Despite these limitations, the scan made in constant height mode does not have large amounts of noise and does not require adjustments of any parameters.

In general, the constant height and constant force modes have been found to be precise and capable of scanning surfaces beyond the diffraction limits of visual microscopes. Although the constant force mode requires sensitive adjustments, it can produce scans of samples with deep structures without damaging the tip or the sample. On the other hand, the constant height mode does not support deep structures but produces high-quality scans with minimal noise and adjustments.

This experiment can be modified and expanded in the future. Repeated scannings and adjustments until the perfect combination is found can establish the precise relation between the P, I, and D values and the quality of the scan obtained in the constant force mode. Moreover, scanning the same surface but in different modes furthers the discussion of distinctions of different scanning modes. The lateral force measurements were briefly mentioned but should have been discussed in great detail. In future, the experiment's focus might be shifted to this scanning mode as it allows the detection of different materials within a single sample. This can later be applied to biology to scan living cells.

References

1. Abramovitz, M., & Davidson, M. W. (n.d.). Numerical Aperture and Resolution. Olympus Lifescience. <https://www.olympus-lifescience.com/en/microscope-resource/primer/anatomy/numaperture/#:~:text=In%20practice%2C%20however%2C%20most%20oil,ranging%20from%201.0%20to%201.35>.
2. Binnig , G., Quate, C. F., & Gerber, C. (1986). Atomic Force Microscope. Phys. Rev. Lett., 56(9), 930-. <https://doi.org/10.1103/PhysRevLett.56.930>
3. B.V. Derjaguin, V.M. Muller, Y.P. Toporov, Effect of contact deformations on the adhesion of particles. J. Colloid Interface Sci. 53, 314 (1975). [https://doi.org/10.1016/0021-9797\(75\)90018-1](https://doi.org/10.1016/0021-9797(75)90018-1)
4. Feigl, D.: Das Rasterkraftmikroskop im Praktikum, Karlsruher Institut für Technologie, state examination paper, 2012
1. Lipson, S. G., Lipson, H., & Tanhauser, D. S. (1995). Optical Physics (3rd ed., pp. 327-340). Cambridge University Press.
2. Sarrid, D. (1994). Scanning Force Microscopy. Oxford University Press.
3. Voigtländer, B. (2019). Atomic Force Microscopy (2nd ed.). Springer Nature Switzerland AG.
4. L. Zitzler, S. Herminghaus, F. Mugele, Capillary forces in tapping mode atomic force microscopy. Phys. Rev. B 66, 155436 (2002). <https://doi.org/10.1103/PhysRevB.66.155436>